Image Analysis of Patient Data from the Hybrid Photoacoustic-Ultrasound Tomography System PAM3

Bruno De Santi[a], Felix Lucka[b], Rianne F.G. Bulthuis[a], Jeroen Veltman[a,c], Margreet van de Schaaf[d], Hendrik Messal[e,f], Mariël Brinkhuis[g], Ben Cox[h], Srirang Manohar*[a]

[a] Multi-Modality Medical Imaging, Tech Med Centre, University of Twente, Enschede, The Netherlands
[b] Computational Imaging Group, Centrum Wiskunde & Informatica, Amsterdam, The Netherlands
[c] Department of Radiology, Ziekenhuisgroep Twente, Hengelo, The Netherlands
[d] Department of Radiology, Medisch Spectrum Twente, Enschede, The Netherlands
[e] Division of Molecular Pathology, The Netherlands Cancer Institute, Amsterdam, The Netherlands
[f] Oncode Institute, Amsterdam, The Netherlands
[g] Laboratory for Pathology East Netherlands, Hengelo, The Netherlands
[h] Department of Medical Physics and Biomedical Engineering, University College London, London, United Kingdom

ABSTRACT

The PAM3 system is a hybrid photoacoustic-ultrasound system for imaging the breast. The ultrasound mode enables extraction of speed-of-sound (SOS) maps that can be used to improve photoacoustic (PA) reconstruction. SOS holds information that can be used potentially for tissue characterization and discrimination. PA computed tomography images were reconstructed using an iterative model-based optimization framework. An image analysis pipeline has been developed to analyze the PA/US images and compare them with contrast-enhanced Magnetic Resonance (ceMR) images. We imaged patients using PAM3 in a study approved by the Medical Ethics Review Board. Patients with a tumor suspicious for malignancy, based on conventional diagnostic imaging, were asked to participate. All patients received X-ray mammography, ultrasound imaging and ceMR imaging. The preliminary results on a patient with a fibroadenoma demonstrate that combining multi-wavelength PA and sound speed imaging is potentially valuable for visualizing breast cancer. From PA we obtain functional information with sound speed providing structural information.

Keywords: breast imaging, photoacoustic tomography, ultrasound tomography, image analysis

1. INTRODUCTION

Breast cancer is a heterogeneous disease with diverse characteristics and clinical manifestations. For this reason, through the clinical pathway, patients undergo different imaging examinations, such as X-ray Mammography (MMG), Ultrasound (US) and Contrast-enhanced Magnetic Resonance (ceMR) imaging, leading to exposure to ionizing radiations, use of contrast agents, therefore high patient burden and clinical costs [1]. In the context of breast cancer, Photoacoustic Tomography (PAT) has shown promising results, being a fast, relatively cheap, and contrast-agent-free functional imaging technique which allows to accurately depict blood vessels [2]. In photoacoustic (PA) imaging, tissue is illuminated with short light pulses in the near-infrared range. With the absorption of light by tissue chromophores, the PA effect takes place which consists of local temperature rise, thermoelastic expansion, pressure build-up and generation of ultrasound waves [3]. In the last decade, multiple PAT systems with different US detection geometries (arc-shaped, ring and hemispherical arrays) and light delivery systems (one or multiple light sources) have been proposed [4], and some of them tested in patients with breast malignancies [2], [5], [6].

The University of Twente, PA Imaging R&D BV, and various partners, were responsible for developing the first three-dimensional (3D) hybrid photoacoustic-ultrasound imaging system (PAM3) [7]. The combination of multispectral PAT and US tomography (UST) allows to obtain a multimodal 3D image of the breast, depicting both anatomical description

Photons Plus Ultrasound: Imaging and Sensing 2025, edited by Alexander A. Oraevsky, Lihong V. Wang, Proc. of SPIE Vol. 13319, 1331902 · © 2025 SPIE
1605-7422 · doi: 10.1117/12.3043362

of the breast (adipose and fibroglandular tissue) and functional information (vascularization and potentially oxygen saturation of blood). The performance of the PAM3 system was evaluated on a set of test objects and in human volunteers which showed the ability of tracking vessels up to 48 mm with an isotropic sub-mm resolution [7]. The PAM3 system has been installed in a Dutch hospital (Medisch Spectrum Twente, Oldenzaal, The Netherlands) and a clinical study is currently being conducted to validate the performance of the system on patients. In this work, we present the methodological approach implemented to analyze patient data and the first preliminary results on a breast lesion.

2. METHODS

PAM3 system

Figure 1 shows a graphical illustration of the PAM3 system and its main compartments. The entire system is embedded in a custom-designed frame with bed-top on which the woman can lie on prone. The breast is inserted through the imaging aperture into a water-filled imaging bowl. The imaging bowl (26 cm inner diameter) is equipped with 512 US transducers for the detection and transmission of US and 40 optical fiber bundle terminations to homogeneously illuminate the breast. The bowl is embedded in a core which contain data acquisition systems and electronics to service the US transducers and produce pulses to trigger the US transmission. During a measurement, the core can rotate around its central axis to acquire multiple projections. Finally, a polyvinylchloride (PVC) cup is used to centralize and stabilize the breast during the measurement [7].

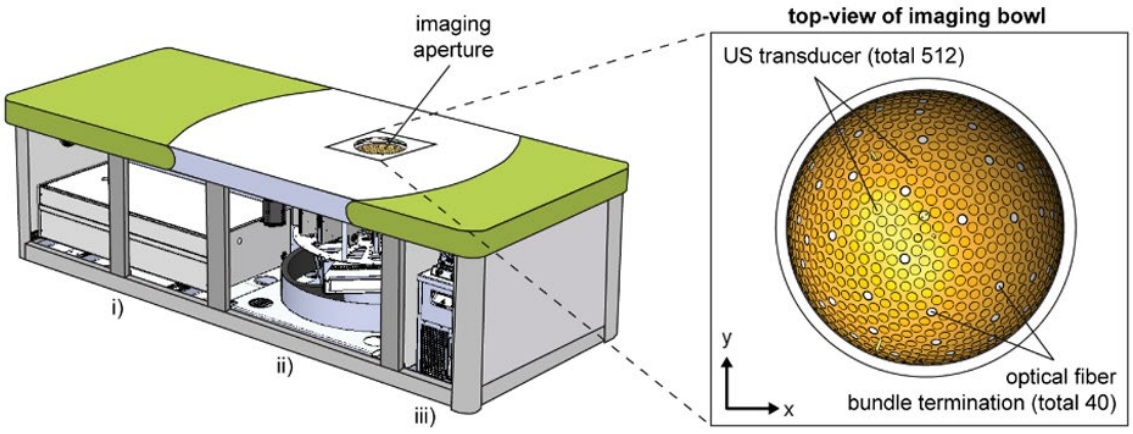

Figure 1. Illustration of the PAM3 system. The systems consists of three main compartments: i) the laser system, ii) rotating core and iii) temperature control unit. The recording aperture is an hemispherical imaging bowl (top-view on the right-hand side of the figure) containing 512 US transducers and 40 optical fiber bundle terminations. Adapted from [7].

Initial clinical demonstration

The system is installed in the Medisch Spectrum Twente hospital in Oldenzaal (Twente, The Netherlands). Figure 2(a) shows a photograph of the device. After informed consent and approved protocol study, a total number of 18 patients were acquired. The imaging protocol takes 5 minutes to acquire PA at five different wavelengths (720, 755, 797, 833, 870 nm) and UST data for a breast. The chosen imaging protocol was fixed after experiments on phantoms and volunteers [7]. PA data and UST data were processed offline to reconstruct the 3D PA images and 3D Speed-of-Sound (SOS) maps. Other conventional images were acquired according to the standard clinical routine: MMG, US and ceMR. Particular attention was given to ceMR, since the use of contrast agent and the volumetric nature of the image allows us to visualize vascular structures in 3D and correlate our PA images to it as reference.

Image reconstruction

PA images were reconstructed using an iterative, model-based reconstruction method [8]. In order to compensate wave aberrations in the acoustic wave propagation model, the measured 3D SOS map of the breast is used in the PA inversion.

The 3D SOS maps were reconstructed from the UST data using for the first time a three-dimensional full-waveform inversion (FWI) algorithm [9].

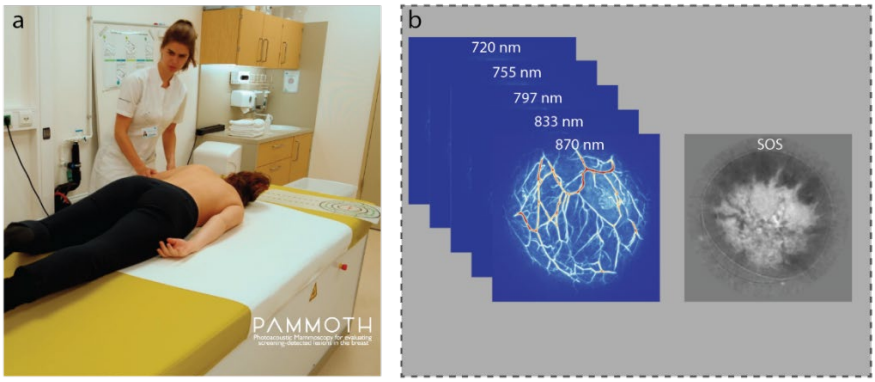

Figure 2. (a) Photograph of the PAM3 system installed in MST hospital in Oldenzaal (Twente, The Netherlands) during a demonstration conducted by an operator (R.F.G.B.) on a volunteer. Snapshot from video available online (https://www.pammoth-2020.eu/symposium2021.html). (b) Output of a patient measurement: five wavelengths PA reconstructions (720, 755, 797, 833 and 870 nm) and SOS map. The PA images shown are maximum intensity projections of the reconstructed PA images. A single slice of the SOS map is shown. Reconstructions were computed offline. The acquisition of the data takes 5 minutes for each breast.

Image analysis

An image analysis pipeline was designed and developed to analyze the PA and SOS images. The pipeline consists of the following steps:

- **Data preparation -** MATLAB files of the PA reconstructions and the SOS reconstruction were converted into Neuroimaging Informatics Technology Initiative (NIFTI) file format**.** The header of the NIFTI files included also information about the image-to-world geometric transformation to allow accurate and user-friendly visualization with available medical imaging software.
- **Tissue segmentation -** Fibroglandular and adipose tissue of the breast were segmented from the 3D SOS maps using a K-means clustering ($k = 3$) on the SOS values. Voxels belonging to the cluster with highest average intensity were classified as fibroglandular tissue, the remaining voxels confined inside the breast were classified as adipose tissue. The skin layer was defined as the most superficial (0.5 mm) layer of the cup mask (a binary mask representing the cup used during the measurement). 3DSlicer was used to fix small errors in the segmentations [10].
- **Optical fluence compensation -** Average optical properties were assigned to each of the segmented compartments (skin, fibroglandular and adipose tissue) [11]. The Monte Carlo eXtreme (MCX) for MATLAB (MCXLAB) toolbox [12] was used to perform the photon transport simulations using a digital twin of the PAM3 light delivery system (modeling the light sources position, the beam geometry and opening angle). Optical fluence maps at the 5 different wavelengths were used to compensate the corresponding PA reconstructions.
- **Data visualization and correlation with ceMR –** An interactive graphical-user-interface was developed on MeVisLab [13] to allow visualization of the PA, SOS and ceMR volumes in form of 3D rendering, 2D slices scrolling, maximum intensity projections, and allows also the annotation of relevant landmarks and regions of interests in the images.

3. RESULTS

In this proceeding a single case will be shown. After self-examination, the patient went to the hospital. X-ray MMG imaging showed a dense and oval mass of 1.4 cm diameter located at 9 o'clock. US evaluation showed a slightly hypoechoic lesion with defined margins. According to the Breast Imaging Reporting and Data System, the lesion was classified as BIRADS 3. In the post contrast T1w MR image, the lesion appeared as an enhanced mass with regular margins

with vasculature associated to it [indicated by the green arrows V1 and V2 in Figure 3(a)]. Diagnosis was made that the lesion was a fibroadenoma. In Figure 3(b), a local coronal maximum intensity projection of the PA image of a 5 mm thick slab of tissue around the tumor is plotted where the same vascular structures pointed in the MR are visible (V1 and V2). Interestingly, what appear to be as capsular vessels which surround the fibroadenoma are seen in the PA image but not on the MR (V3 and V4). Figure 3(c) shows the overlay of SOS and PA images where one can appreciate both morphological and functional information of the lesion.

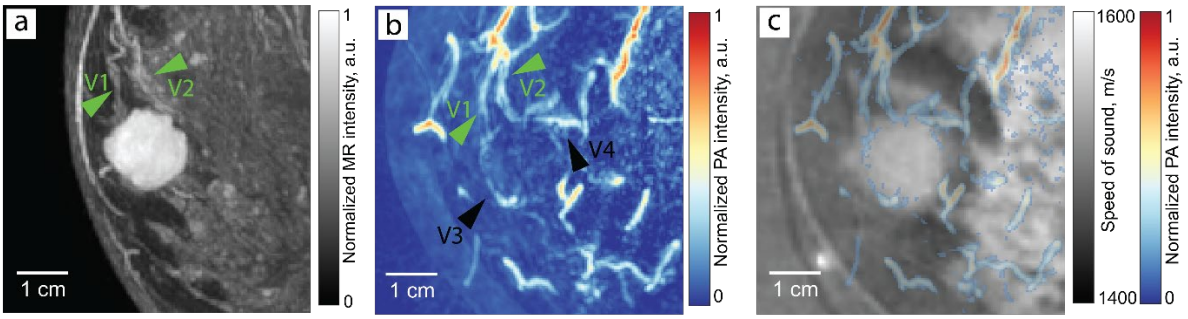

Figure 3. Comparison of ceMR, PA and SOS images of the analyzed patient case. (a) The local maximum intensity projection (coronal view) of a 5 mm thick slab of tissue centered in the tumor of the T1w post contrast MR image shows an enhanced mass with regular margins and the presence of associated vasculature (V1 and V2, green arrows). (b) Local maximum intensity projection of the PA image at 720 nm shows the same associated vascular structures present in MR (V1 and V2, green arrows) and also capsular vessels surrounding the fibroadenoma (V3 and V4, black arrows). (c) The central slice of the SOS map shows higher SOS value than adipose tissue in the region but does not clearly show the shape of the lesion. (d) The overlay of PA and SOS can potentially show both morphological and functional information about the lesion.

4. DISCUSSION AND CONCLUSIONS

We demonstrated the use of a 3D hybrid photoacoustic/ultrasound system in a clinical case. PA was able to show the associated tumor vasculature (similarly to what shown in previous studies [5]). The first 3D full-wave-inversion SOS reconstructions are highly promising as they clearly show the location of the lesion. The PA image shows a rim signal surrounding the fibroadenoma which is not observed in the ceMR image. The fibroadenoma also appears as high contrast region in contrast-enhanced MR. The rim signal may be an imaging feature in PA presentation of fibroadenoma. The next steps are to identify a well-defined set of PA imaging biomarkers associated with various types of breast abnormalities. More patient data is being analyzed with the image analysis pipeline in order to gain more insights. In the near future, new patient results will be finalized and published.

ACKNOWLEDGEMENTS

This study was funded by:

- **EFRO**: OOST-00103 Elastografie voor snellere herkenning van borstkanker in 3D fotoakoestische mammografie
- **Horizon 2020's research and innovation program:** H2020 ICT 2016-2017, under grant agreement No732411, initiative of the Photonics Public Private Partnership
- **REACT-EU:** Foto-akoestische mammografie naar de kliniek met de PAM3+
- **PIHC:** Fotoakoestieke tomografie van de borst: De weg naar monitoren van neo-adjuvant chemotherapie

Authors thank Rutger Pompe van Meerdervoort, Laurens Alink, Martin Nanninga, Tim op't Root and Wouter Muller-Kobolt from PA Imaging R&D BV. Further Maura Dantuma and Lioe-Fee de Geus Oei are thanked for their early work on the project and for arranging the Medical Ethics study protocol. Authors also express all other members of the PAMMOTH consortium for their contributions within the project.

REFERENCES

[1] M. M. Voets et al., "Diagnostics in patients suspect for breast cancer in The Netherlands," Current Oncology, vol. 28, no. 6, pp. 4998–5008, Dec. 2021, doi: 10.3390/CURRONCOL28060419/S1.

[2] L. Lin et al., "Single-breath-hold photoacoustic computed tomography of the breast," Nat Commun, vol. 9, no. 1, p. 2352, Dec. 2018, doi: 10.1038/s41467-018-04576-z.

[3] Y. Zhou, J. Yao, and L. V. Wang, "Tutorial on photoacoustic tomography," J Biomed Opt, vol. 21, no. 6, p. 061007, 2016, doi: 10.1117/1.jbo.21.6.061007.

[4] S. Manohar and M. Dantuma, "Current and future trends in photoacoustic breast imaging," Photoacoustics, vol. 16, no. April, p. 100134, 2019, doi: 10.1016/j.pacs.2019.04.004.

[5] M. Toi et al., "Visualization of tumor-related blood vessels in human breast by photoacoustic imaging system with a hemispherical detector array," Sci Rep, vol. 7, no. 1, p. 41970, Feb. 2017, doi: 10.1038/srep41970.

[6] S. M. Schoustra et al., "Imaging breast malignancies with the Twente Photoacoustic Mammoscope 2," PLoS One, vol. 18, no. 3, p. e0281434, Mar. 2023, doi: 10.1371/journal.pone.0281434.

[7] M. Dantuma et al., "Fully three-dimensional sound speed-corrected multi-wavelength photoacoustic breast tomography," Aug. 13, 2023. doi: arXiv:2308.06754.

[8] S. Arridge et al., "Accelerated high-resolution photoacoustic tomography via compressed sensing," Phys Med Biol, vol. 61, no. 24, pp. 8908–8940, Dec. 2016, doi: 10.1088/1361-6560/61/24/8908.

[9] F. Lucka, M. Pérez-Liva, B. E. Treeby, and B. T. Cox, "High resolution 3D ultrasonic breast imaging by time-domain full waveform inversion," Inverse Probl, vol. 38, no. 2, p. 025008, Dec. 2021, doi: 10.1088/1361-6420/AC3B64.

[10] A. Fedorov et al., "3D Slicer as an image computing platform for the Quantitative Imaging Network," Magn Reson Imaging, vol. 30, no. 9, pp. 1323–1341, Nov. 2012, doi: 10.1016/j.mri.2012.05.001.

[11] S. L. Jacques, "Optical properties of biological tissues: a review," Phys Med Biol, vol. 58, no. 11, Jun. 2013, doi: 10.1088/0031-9155/58/11/R37.

[12] L. Yu Fanny Nina-Paravecino David Kaeli Qianqian Fang Leiming Yu, F. Nina-Paravecino, and D. Kaeli, "Scalable and massively parallel Monte Carlo photon transport simulations for heterogeneous computing platforms," vol. 23, no. 1, p. 010504, Jan. 2018, doi: 10.1117/1.JBO.23.1.010504.

[13] F. Ritter et al., "Medical image analysis," IEEE Pulse, vol. 2, no. 6, pp. 60–70, Nov. 2011, doi: 10.1109/MPUL.2011.942929.